The effect of a Gaussian distribution of chain-lengths on the phase-behaviour of a model system of rod-like macromolecules in solution

J. K. Moscicki* and G. Williams
Edward Davies Chemical Laboratories, University College of Wales, Aberystwyth, Dyfed, SY23 1NE, UK
(*Received* 3 *September* 1981)

The calculations of Flory and co-workers for the formation and composition of isotropic, bi-phasic and anisotropic systems composed of rod-like macromolecules in solution have been extended to include a Gaussian distribution of rod-lengths. The critical concentrations for the beginning and end of the bi-phasic range v_p^{0*} and v_p^{0**} respectively, the volume fraction of anisotropic phase Φ_A, the compositions and average molecular weights of isotropic and anisotropic phases, and the order parameter S of the anisotropic phase are calculated as a function of polymer concentration v_p^0 for rod-length x_0 in the range 30 to 70 and for a Gaussian distribution half-width $\Delta_{\frac{1}{2}}$ in the range 10 to 70. The extent of the bi-phasic range and the composition of the two components is found to be strongly dependent on the breadth of the distribution and average rod-length. The applicability of the calculations to data for poly(alkylisocyanates) in solution is briefly considered.

Keywords Macromolecules; chain-length; Gaussian distribution; phase-behaviour; isotropic phase; anisotropic phase

INTRODUCTION

In an important series of papers, Flory and co-workers have given theoretical treatments of the thermodynamic behaviour of rod-like particles in solution[1-8]. In a recent series[3-6] they extended the theory to polydisperse systems having 'most-probable'[5] and Poisson[6] distributions of chain length. Related treatments have recently been given by Dieblieck and Lekkerkerker[9] and by Doi[10]. The important feature of such theoretical treatments is that it is predicted that as the concentration of polymer is increased the system goes sequentially through the isotropic phase to a biphasic material, in which isotropic and 'anisotropic' phases coexist, to a wholly 'anisotropic' phase. Here the 'anisotropic' phase is organized in a manner similar to that of a nematic liquid-crystal phase. Such phase behaviour is well-known for certain polypeptides and aromatic polyamides in solution (for key references see ref. 2, refs. 2–8). Whilst the interest in lyotropic liquid-crystalline systems composed of rod-like molecules such as poly-γ-benzyl-L-glutamate goes back twenty five years to the classic work of Conmar Robinson and co-workers[11,12] more recent studies of aromatic polyamides[13,14] and polyesters[15], which form high modulus fibres or thermoplastics have revived interest in this class of polymer solutions, and have stimulated much current activity. In particular, Aharoni and Walsh[16,17] showed that certain poly(alkylisocyanates) formed lyotropic liquid-crystal materials when dissolved in such solvents as chloroform or toluene at polymer concentrations exceeding about 15% (w/w). The formation of bi-phasic and lyotropic-nematic phases for these polymers was in general accord with the predictions of Flory and co-workers, and one special feature was the observation of partial fractionation of a polydisperse sample between the two phases, as predicted by theory[3-6]. Aharoni and co-workers have made extensive studies of lyotropic and thermotropic systems involving poly(alkyliosocyanates)[16-23]. Since these polymers have extremely large electric dipole moments[24], the dielectric technique is able to provide a ready means of studying the structure and dynamics of their isotropic, bi-phasic and lyotropic-nematic solutions. Extensive studies of fairly dilute isotropic solutions of the n-butyl, n-hexyl, n-octyl isocyanate polymers have been made using dielectric[24-30] and Kerr-electro-optical[29-31] techniques and such information as the mean-square dipole moment, effective relaxation time, and their dependencies upon molecular weight, concentration and temperature, have been well documented and explained in molecular terms. Quite recently Moscicki and co-workers[32,33] have reported studies of the dielectric relaxation of a sample of poly(n-hexylisocyanate) and a copolymer of n-butyl and n-nonyl isocyanate over a wide range of concentration, in toluene, to include isotropic, bi-phasic and lyotropic-nematic (anisotropic) phases. It was shown that as the polymer concentration c_p was increased in the isotropic range both the magnitude ($\Delta\varepsilon$) and average relaxation time ($\langle\tau\rangle$) increased monotonically, but both quantities showed a marked decrease with increasing c_p in the bi-phasic range, tending to approximately constant values in the wholly anisotropic phase. In view of this interesting but complicated behaviour it seemed desirable to obtain information about the relative amounts of isotropic (I)

* Permanent address: Institute of Physics, Jagellonian University, ul-Reymonta 4, 30–59, Krakow, Poland

0032-3861/82/040558-11$03.00

and anisotropic (A) phases, and their compositions, in the bi-phasic range and to estimate the effective polymer concentrations at which the bi-phasic material appears and terminates. The theory of Flory and co-workers[1-8] is ideal for this purpose. Their calculations refer to the special cases of the 'most-probable' and Poisson distributions of rod-length whose contours are fixed for a given average rod-length. For poly(n-butylisocyanate) Bur and Fetters[34] found that fractions had approximately symmetrical distributions of molecular weight. Thus it seemed appropriate to calculate the phase-behaviour of rod-like particles in solution using the Flory theory for the case of a normal (or Gaussian) distribution of rod-length. In addition, it is possible to vary the width of the Gaussian curve for a given average rod-length so we may extend the work of Flory and co-workers to include the variable of polydispersity. A preliminary account of our work has been given[35] and its qualitative application to the dielectric relaxation behaviour of the butyl-nonyl isocyanate copolymer[37] and poly(n-hexylisocyanate)[32,36] has been considered. The present paper gives the detailed account of our extensive calculations for the case of a Gaussian distribution of rod-lengths.

THEORY

The model is exactly that developed by Flory and his co-workers[1-7], and the reader should consult those works, especially refs. 4–7 for the case of a distribution of rod-lengths. For the present work,* the Gaussian distribution leads to the following relation

$$\frac{n_x^0}{n_p^0}=\exp\left(-4(\ln 2).\left[\frac{x-x_0}{\Delta^1_{\frac{1}{2}}}\right]^2\right)\equiv P(x) \qquad (1)$$

The superscript '0' indicates here, and throughout, the unpartitioned distribution so n_x^0 is the number of x-meric species in the total volume V and n_p^0 is the number of solute particles in the volume V. x denotes the number of units in a chain and the axis-ratio in that chain[3-6]. For simplicity the solvent particles are assumed to have unit dimension[3-6].

The volume-fraction ratio is given by

$$\frac{v_x^0}{v_p^0}=\frac{xn_x^0}{\sum_1^\infty xn_x^0}=\frac{xP(x)}{\sum_1^\infty xP(x)}=\frac{xP(x)}{\bar{x}_p^0} \qquad (2)$$

v_x^0 and v_p^0 are the volume-fraction of x-meric species and of total polymer, respectively, in the volume V.

Let v_p and v'_p denote the volume-fractions of total solute in the isotropic (I) and anisotropic (A) phases, respectively. (Primed quantities indicate the A-phase and unprimed quantities the I-phase[3-6]). Then

$$\Phi_A v'_p+(1-\Phi_A)v_p=v_p^0 \qquad (3)$$

Φ_A is the volume-fraction of the anisotropic phase for a given value of v_p^0. Note that $(1-\Phi_A)$ is the volume-fraction of the isotropic phase. Also

$$\Phi_A v'_x+(1-\Phi_A)v_x=v_x^0 \qquad (4)$$

From equations (2) and (3)

$$\Phi_A\frac{v'_x}{v_p^0}+(1-\Phi_A)\frac{v_x}{v_p^0}=\frac{x}{\bar{x}_p^0}P(x) \qquad (5)$$

Conservation of the total number of molecules requires that

$$\Phi_A\frac{v'_p}{\bar{x}'_p}+(1-\Phi_A)\frac{v_p}{\bar{x}_p}=\frac{v_p^0}{\bar{x}_p^0} \qquad (6)$$

$\bar{x}_p$ and $\bar{x}'_p$ are the number-average lengths of solute particles in I and A phases respectively. Following Flory[2], for equilibrium between I and A phases we must have

$$\frac{v'_x}{v_x}=\exp(x[\eta-2/y]) \quad : \text{ for species } x\leqslant y \qquad (7a)$$

$$\frac{v'_x}{v_x}=\left(\frac{y}{ex}\right)^2\exp(\eta x) \quad : \text{ for species } x>y \qquad (7b)$$

y is a disorder parameter[1] defined as $y=x\sin\theta_x$, where θ_x is the angle between the order direction and the long axis of the rod-like particle. η is given by

$$\eta=\frac{2}{y}+\ln\left(\frac{1-v'_p}{1-v_p}\right) \qquad (8a)$$

or

$$\eta=v_2\left(1-\frac{1}{\bar{x}_p}\right)-v'_R\left(1-\frac{1}{\bar{x}'_R}\right)+v'_A(1-y)\frac{1}{\bar{x}'_A} \qquad (8b)$$

subscripts 'A' and 'R' distinguish species in 'aligned' and 'random' states within the anisotropic phase.

The condition of equilibrium requires that equations (5) and (7) to be simultaneously fulfilled and so combination and rearrangement lead to the following:

$$\frac{v'_x}{v_p^0}=\frac{1}{(1-\Phi_A)\bar{x}_p^0}\cdot\frac{xP(x)}{\left[\exp\left(x\left[\frac{2}{y}-\eta\right]\right)+\Phi_A/(1-\Phi_A)\right]} \quad : x\leqslant y \qquad (9a)$$

$$\frac{c'_x}{v_p^0}=\frac{1}{(1-\Phi_A)\bar{x}_p^0}\left(\frac{y}{e}\right)^2\frac{xP(x)}{[x^2(\exp(-\eta x)]+y^2\Phi_A/(1-\Phi_A)e^2]} \quad : x>y \qquad (9b)$$

and, by definition

$$\frac{v'_R}{v_p^0}=\sum_{x=1}^{x\leqslant y}\left(\frac{v'_x}{v_p^0}\right)=\frac{1}{(1-\Phi_A)\bar{x}_p^0}\cdot\sum_{x=1}^{x\leqslant y}\frac{xP(x)}{\left[\exp\left(x\left(\frac{2}{y}-\eta\right)\right)+\Phi_A/(1-\Phi_A)\right]} \qquad (10a)$$

* Owing to the large number of terms for the model involved in this work, a Glossary of Terms is appended. Further information is given in refs. 2–6

$$\frac{v'_A}{v_p^0}=\sum_{x>y}\left(\frac{v'_x}{v_p^0}\right)=\frac{1}{(1-\Phi_A)\bar{x}_p^0}\cdot\left(\frac{y}{e}\right)^2\sum_{x>y}\frac{xP(x)}{[x^2\exp(-\eta x)+y^2\Phi_A/(1-\Phi_A)e^2]} \quad (10b)$$

The number-average length of the rods in the anisotropic phase will be

$$\bar{x}'_R=\left[\sum_{x=1}^{x\leq y}\frac{xP(x)}{\left[\exp\left(x\left(\frac{2}{y}-\eta\right)\right)+\Phi_A/(1-\Phi_A)\right]}\right]\times\left[\sum_{x=1}^{y}\frac{P(x)}{\left[\exp\left(x\left(\frac{2}{y}-\eta\right)\right)+\Phi_A/(1-\Phi_A)\right]}\right]^{-1} \quad (11a)$$

for the 'random' state and

$$\bar{x}'_A=\left[\sum_{x>y}\frac{xP(x)}{[x^2\exp(-\eta x)+y^2\Phi_A/(1-\Phi_A)e^2]}\right]\times\left[\sum_{x>y}\frac{P(x)}{[x^2\exp(-\eta x)+y^2\Phi_A/(1-\Phi_A)e^2]}\right]^{-1} \quad (11b)$$

for the 'aligned' state.

The following equations must also be valid

$$\frac{v'_p}{v_p^0}=\frac{v'_R}{v_p^0}+\frac{v'_A}{v_p^0} \quad (12)$$

$$\frac{v'_p}{\bar{x}'_p}=\frac{v'_R}{\bar{x}'_R}+\frac{v'_A}{\bar{x}'_A} \quad (13)$$

This last equation enables $\bar{x}'_p$ to be determined. The equilibrium value of y obeys the relation

$$v'_A=[1-\exp(-2/y)].[1-y/\bar{x}'_A]^{-1} \quad (14)$$

From equation (6) we may write

$$v_p^0=[\{\exp((2/y)-\eta)\}-1].[\{v'_p\exp((2/y)-\eta)-v_p\}/v_p^0]^{-1} \quad (15)$$

This completes the set of equations required to solve the problem.

For a given distribution function $P(x)$ for any value of Φ_A in the range 0 to 1 the values of y and η are calculated following the basic rules:—

(1) For any value of y, the difference between v'_A calculated from equations (14) and (10b) must be zero within a prescribed limit. This is achieved by varying the parameter η.

(2) The difference between the current value of y and that calculated from equation (8b) must be zero within a prescribed limit. This is achieved by varying the current value of y, but still fulfilling requirement (1).

In order to calculate an order parameter useful for future applications of this work, we define the nematic order parameter S as

$$S=\sum_{x>y}S_x\left(\frac{v'_x}{v'_A}\right)=\sum_{x>y}\left(1-\frac{3}{2}\langle\sin^2\theta_x\rangle\right)\frac{v'_x}{v'_A} \quad (16)$$

In order to calculate quantities useful for the restricted small-step angular diffusion of rods, as envisaged in the model of Warchol and Vaughan[37] and Wang and Pecora[38] we assume that the space available to the rod-like particle is restricted to a cone of angle θ_x^0 about the order-direction. The orientation of x-meric species is assumed to be randomly distributed within the cone giving an average $y=x\langle\sin\theta_x\rangle$. Thus

$$\frac{y}{x}=\langle\sin\theta_x\rangle=\frac{\int_0^{\theta_x^0}\sin^2\theta_x d\theta_x}{\int_0^{\theta_x^0}\sin\theta_x d\theta_x}=\frac{\frac{1}{2}[\theta_x^0-(1/2)\sin 2\theta_x^0]}{[1-\cos\theta_x^0]} \quad (17)$$

and

$$\langle\sin^2\theta_x\rangle=\frac{\int_0^{\theta_x^0}\sin^3\theta_x d\theta_x}{\int_0^{\theta_x^0}\sin\theta_x d\theta_x}=\frac{1}{3}[2-(\cos\theta_x^0)(1+\cos\theta_x^0)] \quad (18)$$

Thus

$$S_x=\cos\theta_x^0(1+\cos\theta_x^0)/2 \quad (19)$$

Equation (17) yields θ_x^0 for given (y,x) pairs and each value can be used in equation (19) to give S_x and ultimately S from equation (16).

All calculations were made using the College Honeywell 6080 computer. The accuracy of the values obtained from the computer calculations was 10^{-38}. The calculations for step (1) above proceeded until the difference between both values of v'_A was less than 10^{-4}, whilst for step (2) the difference between the current (or trial) value of y and that calculated was less than 10^{-4} as well. The maximum value of x in the distribution given in equation (2), i.e. x_{max}, was found independently for each case, increasing x_{max} until the values of all parameters calculated by the procedure became constant, independent of x_{max} within an accuracy of 10^{-4}.

Calculations 'A'

We fix the maximum of $P(x)$ at $x_0=50$ and vary the width of the distribution of rod-lengths by varying $\Delta_{\frac{1}{2}}$ from 10 to 70. The corresponding plots of (v_x^0/v_p^0) against x (see equation (2)) are shown in *Figure 1*. Note that the peak in (v_x^0/v_p^0) moves to higher x as $\Delta_{\frac{1}{2}}$ increases, as required by equation (2) since $P(x)$ is multiplied by x.

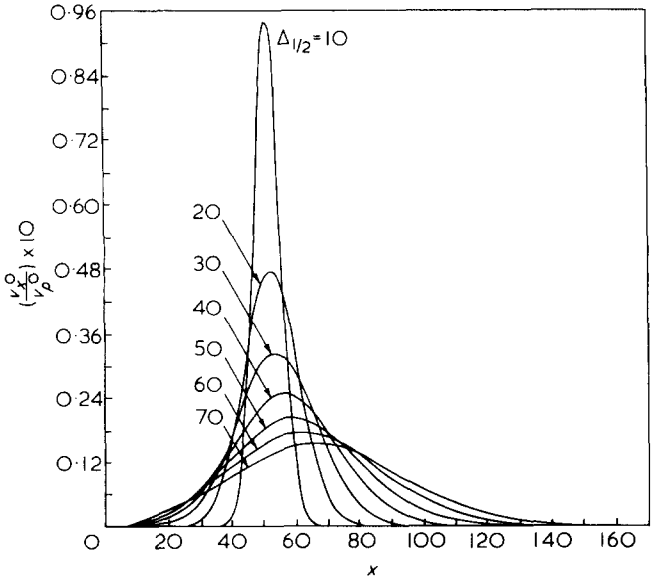

Figure 1 (v_x^0/v_p^0) against rod-length x for x_0 = 50 and $\Delta_{\frac{1}{2}}$ equal to 10, 20, 30, 40, 50, 60 and 70

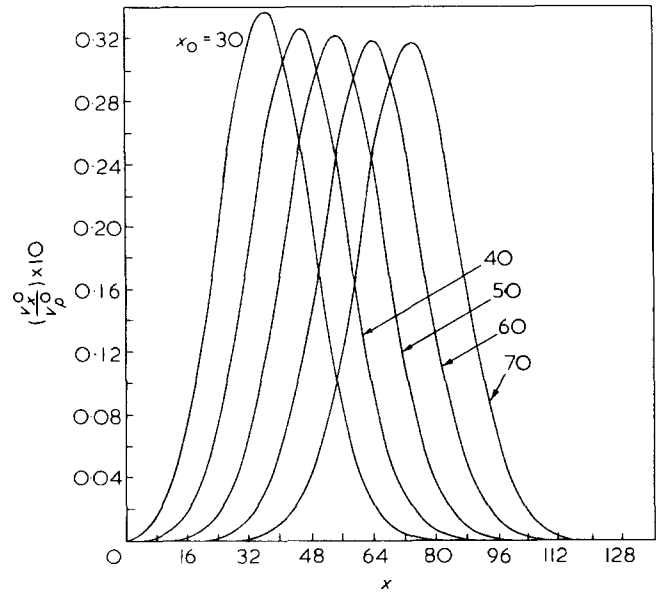

Figure 2 (v_x^0/v_p^0) against rod-length x for $\Delta_{\frac{1}{2}}$ = 30 and x_0 equal to 30, 40, 50, 60 and 70

Calculations 'B'

We fix $\Delta_{\frac{1}{2}}$ at 30 and vary the average rod-length by varying x_0 from 30 to 70. The plots of (v_x^0/v_p^0) against x are shown in *Figure 2*.

Calculations 'C'

We fix $\Delta_{\frac{1}{2}}$ in proportion to x_0 by setting, as our example, $\Delta_{\frac{1}{2}}=2x_0/3$ and vary x_0 from 30 to 70. Plots of (v_x^0/v_p^0) against x are shown in *Figure 3*.

For these calculations the following quantities have been obtained as a function of v_p^0, the volume fraction of polymer in the total volume V: Φ_A, v_p', v_p, y, S, $\bar{x}_p'$, $\bar{x}_p$, $(\bar{x}_p'/\langle x_p'\rangle)$ and $(\bar{x}_p/\langle x_p\rangle)$. The results are presented in that order for calculations A, B and C. Before discussing the results in detail we note the following.

First, v_p' and v_p, $\bar{x}_p'$ and x_p, $\bar{x}_p'/\langle x_p'\rangle$ and $x_p/\langle x_p\rangle$ are drawn in pairs on each figure, and are distinguished by means of symbols placed at the beginning and end of each curve. Open symbols denote the isotropic phase and closed symbols denote the anisotropic phase. A simple example is the data of *Figure 5*. Each curve is calculated for given $(x_0, \Delta_{\frac{1}{2}})$. It must be noticed that for the plots of v_p' and v_p against v_p^0, all v_p lines (lower curves) start and all v_p' lines (upper curves) finish on a straight line which is the diagonal of the corrdinate frame, e.g. in *Figure 12* we show this as the broken line. This is a consequence of the fact that for $v_p^0 \leqslant v_p^{0*}$, where v_p^{0*} is the minimum value of v_p^0 for the appearance of the anisotropic phase (i.e. the start of the bi-phasic range), $v_p = v_p^0$ whilst for $v_p^0 > v_p^{0**}$, where v_p^{0**} is the value of v_p^0 at the end of the bi-phase range (i.e. $\Phi = 1.0$ for $v_p^0 > v_p^{0**}$) we have $v_p' = v_p^0$, independent of the values of x_0 and $\Delta_{\frac{1}{2}}$. Thus the isotropic and anisotropic phase data obey the equation for the diagonal line with

$$v_p = v_p^0 \quad : \quad v_p^0 \leqslant v_p^{0*} \tag{20a}$$

$$v_p = v_p^0 \quad : \quad v_p^0 \geqslant v_p^{0**} \tag{20b}$$

The distribution functions f_x and f_x' (see refs. 1–6) for species partitioned into isotropic and anisotropic phases are defined as follows

$$f_x = (1 - \Phi_A) v_x / v_p^0 \tag{21a}$$

$$f_x' = \Phi_A v_x' / v_p^0 \tag{21b}$$

and of course $P(x) = (f_x + f_x')$. These quantities give the total amounts of x-meric species in the isotropic and anisotropic phases for a given v_p^0. Plots of f_x and f_x' will be shown for given $(x_0, \Delta_{\frac{1}{2}})$ values as a function of v_p^0.

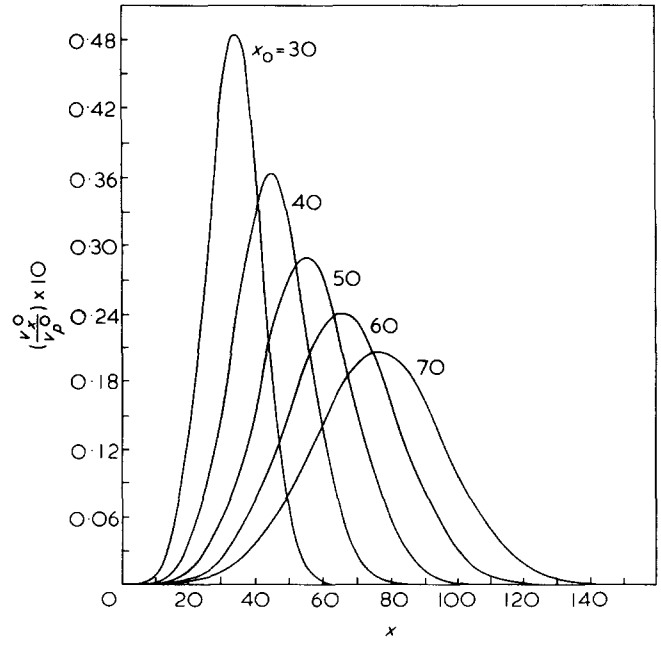

Figure 3 (v_x^0/v_p^0) against rod-length x for $\Delta_{\frac{1}{2}} = (2x_0/3)$ and x_0 equal to 30, 40, 50, 60 and 70

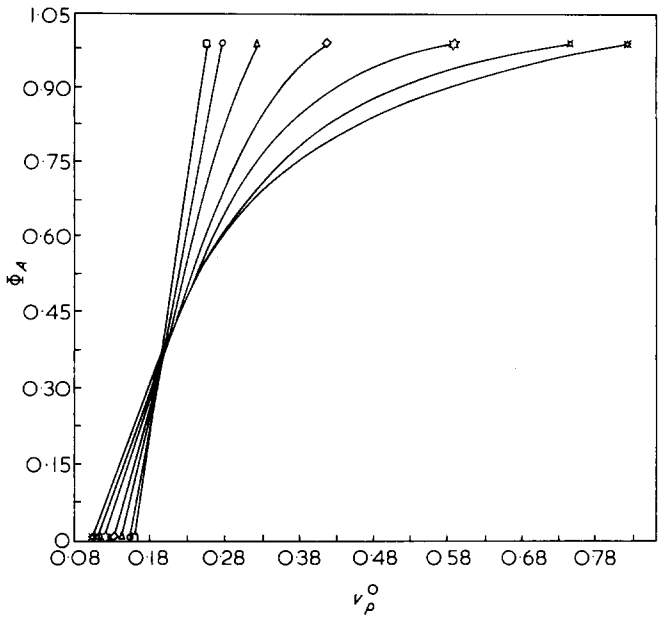

Figure 4 Φ_A against v_p^0 for calculations 'A'. $x_0 = 50$. Lines with extrema as □, ○, △, ◇, ☆, ⊠ and * correspond to $\Delta_{\frac{1}{2}}$ equal to 10, 20, 30, 40, 50, 60 and 70 respectively. Each line gives the bi-phasic range for given $(x_0, \Delta_{\frac{1}{2}})$ pairs. The symbol at low v_p^0 gives v_p^{0*} and the symbol at higher v_p^0 gives v_p^{0**} for that line

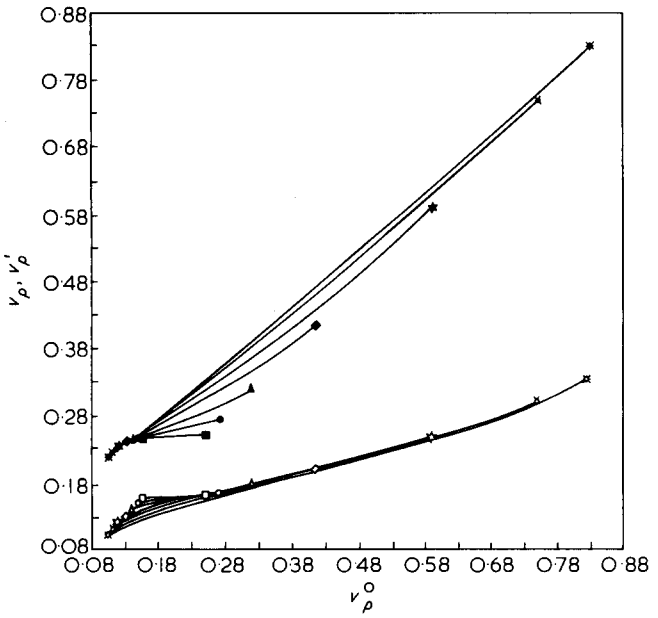

Figure 5 v_p and v_p' against v_p^0 for calculations 'A'. $x_0 = 50$. Lines with extrema as open and filled symbols correspond to isotropic and anisotropic phases respectively. The key is as for *Figure 4*, e.g. the data □——□ refer to the isotropic phase in the bi-phasic material for $\Delta_{\frac{1}{2}} = 10$ whilst the data ◆——◆ refer to the anisotropic phase in the biphasic material for $\Delta_{\frac{1}{2}} = 40$. Each line gives the bi-phasic range for given $(x_0, \Delta_{\frac{1}{2}})$ pairs. The symbol at low v_p^0 thus indicates v_p^{0*} and the symbol at higher v_p^0 indicates v_p^{0**}

RESULTS

Calculations 'A'

As indicated above these calculations give information on the phase behaviour for a system of constant average rod-length x_0 but with varying breadth $\Delta_{\frac{1}{2}}$ of the distribution. *Figures 4–10* summarize the results.

In *Figure 4* $\Phi_A = 0$ for the isotropic phase range, $0 < \Phi_A \leqslant 1$ for the bi-phasic range and $\Phi_A = 1$ for the wholly anisotropic phase range. For $\Delta_{\frac{1}{2}} = 10$, Φ_A increases rapidly for $v_p^0 > v_p^{0*}$ yielding only a narrow range for the bi-phasic material. As $\Delta_{\frac{1}{2}}$ is successively increased in steps of 10 to $\Delta_{\frac{1}{2}} = 70$ it is seen (i) that v_p^{0*} decreases (ii) that the range for the bi-phasic material is remarkably increased (iii) that whilst for narrow distributions the plot Φ_A – vs. – v_p^0 is approximately linear, for $\Delta_{\frac{1}{2}}$ large the plot becomes

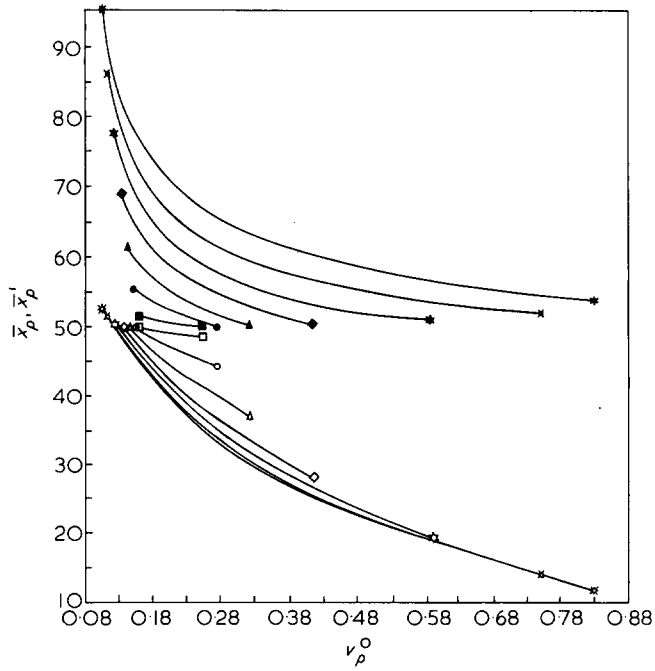

Figure 6 $\bar{x}_p$ and $\bar{x}_p'$ against v_p^0 for calculations 'A'. The lines are constructed, and the notation is the same, as for *Figure 5*. e.g. □——□ refers to the isotropic phase in the bi-phasic material for $\Delta_{\frac{1}{2}} = 10$, whilst ●——● refers to the anisotropic phase in the bi-phasic material for $\Delta_{\frac{1}{2}} = 20$

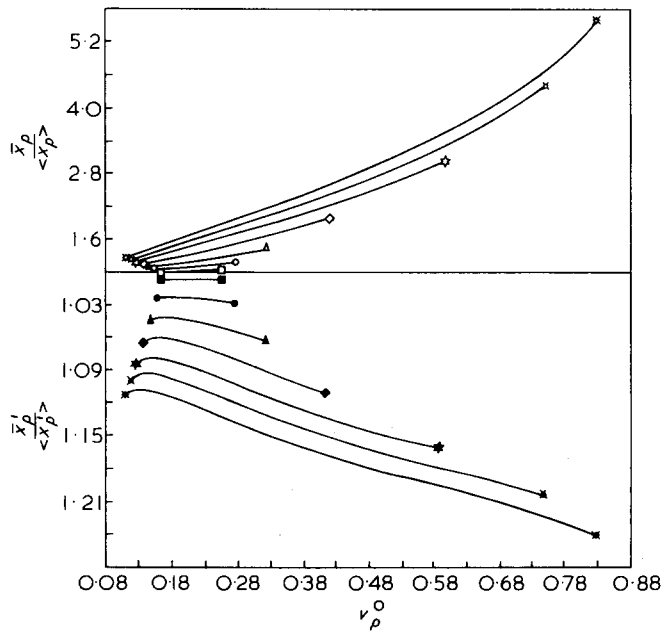

Figure 7 $(\bar{x}_p/\langle x_p \rangle)$ and $(\bar{x}_p'/\langle x_p' \rangle)$ against v_p^0 for calculations 'A'. The lines are constructed as for *Figures 5* and *6*, so the upper and lower data refer to isotropic and anisotropic phases, respectively, in the bi-phasic material

increasingly curved (iv) there is a value of v_p^0 at which Φ_A is approximately independent of the width of the distribution. *Figure 5* shows v_p and v'_p in the bi-phasic range. Note that in the wholly isotropic and wholly anisotropic ranges v_p and v'_p follow equations (20), as discussed above. We note that $v'_p > v_p$, as expected from the works of Flory[1-6], in the bi-phasic range. As the distribution is broadened v_p and v'_p for $v_p^0 = v_p^{0*}$ decrease, the decrease being larger for v_p (i.e. for the isotropic phase). For the bi-phasic range v_p and v'_p increase with v_p^0, the increase in v'_p being much the greater of the two for a given $\Delta_{\frac{1}{2}}^1$. *Figure 6* shows the number-average quantities $\bar{x}_p$ and $\bar{x}'_p$ as a function of v_p^0 and $\Delta_{\frac{1}{2}}^1$. As v_p^0 is increased for constant $\Delta_{\frac{1}{2}}^1$ both quantities decrease. At the critical value $v_p^0 = v_p^{0*}$, $\bar{x}_p \simeq 50$ for all $\Delta_{\frac{1}{2}}^1$, since for $v_p^0 \rightarrow v_p^{0*}$ on the isotropic side of the transition from isotropic to bi-phasic material $\bar{x}_p^0 \simeq 50$. For v_p^0 slightly greater than v_p^{0*} we see that $\bar{x}'_p > 50$, and increases its value with increasing $\Delta_{\frac{1}{2}}^1$. This shows that the high molecular weight species in the distribution dominate the composition of the anisotropic phase within the bi-phasic material when Φ_A is small (see *Figure 4*), and on broadening the distribution selective partitioning of the high molecular species into the anisotropic phase is increased. On increasing v_p^0 both $\bar{x}_p$ and $\bar{x}'_p$ fall, the latter falling to ~ 50 as Φ_A approaches unity. In this higher range the low molecular weight

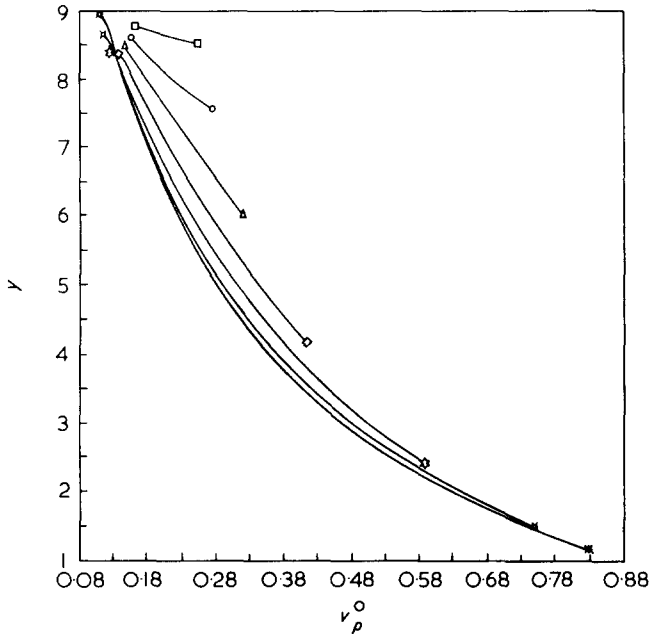

Figure 8 y against v_p^0 for calculations 'A'. The lines are constructed as in *Figure 4*. e.g. ◇——◇ corresponds to $\Delta_{\frac{1}{2}}^1 = 40$

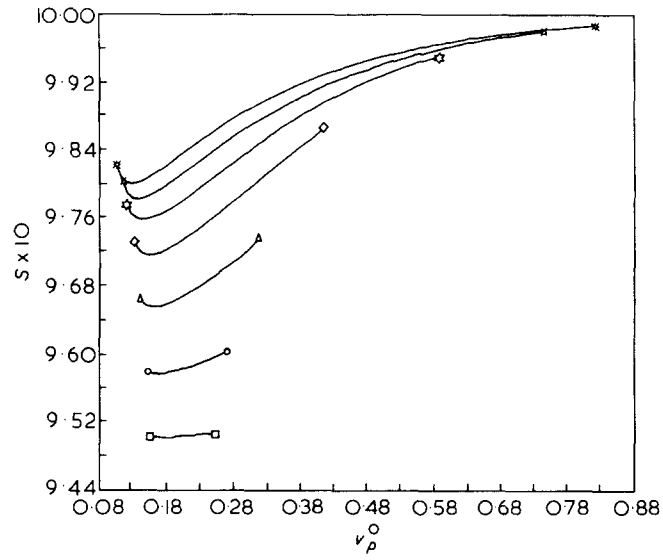

Figure 9 S against v_p^0 for calculations 'A'. The lines are constructed as in *Figure 4*. e.g. ○——○ correspond to $\Delta_{\frac{1}{2}}^1 = 20$

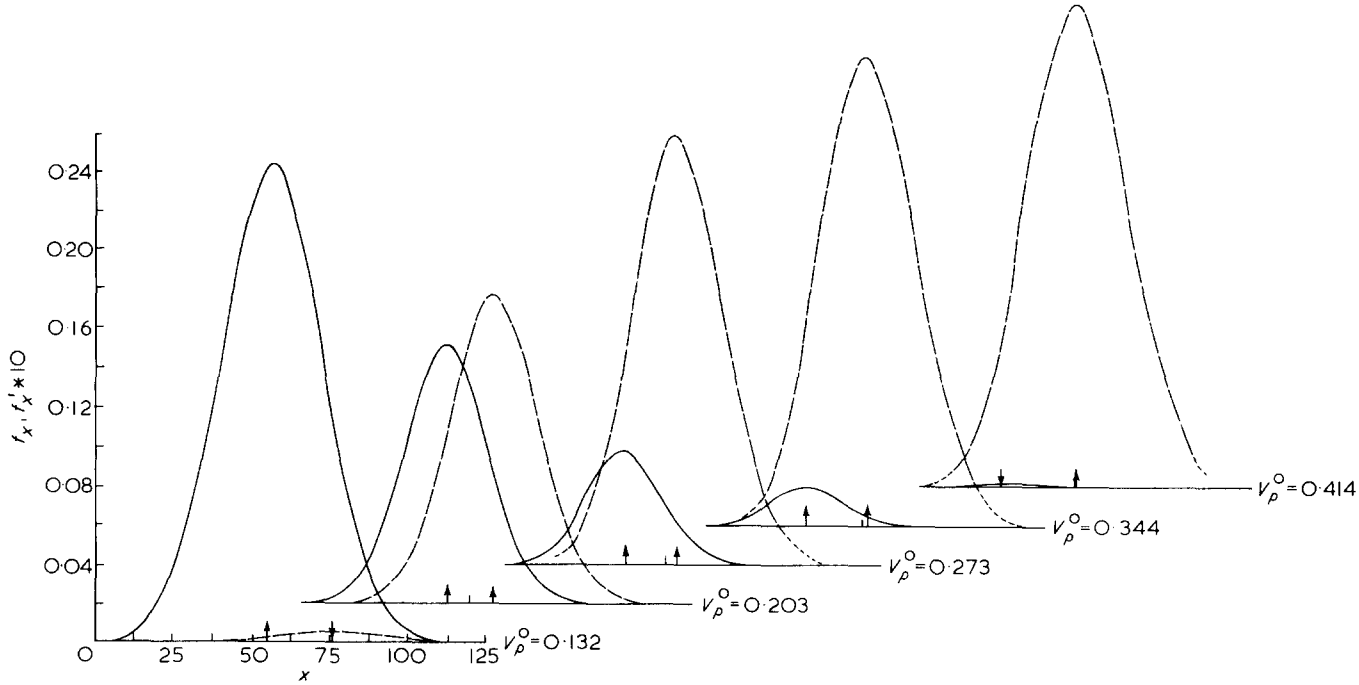

Figure 10 f_x (continuous line) and f'_x (broken line) against x for $x_0 = 50$, $\Delta_{\frac{1}{2}}^1 = 40$. Successive plots from left to right refer to v_p^0 equal to 0.132 (Φ_A = 0.010), 0.203 (Φ_A = 0.350), 0.273 (Φ_A = 0.704), 0.344 (Φ_A = 0.888) and 0.414 (Φ_A = 0.990)

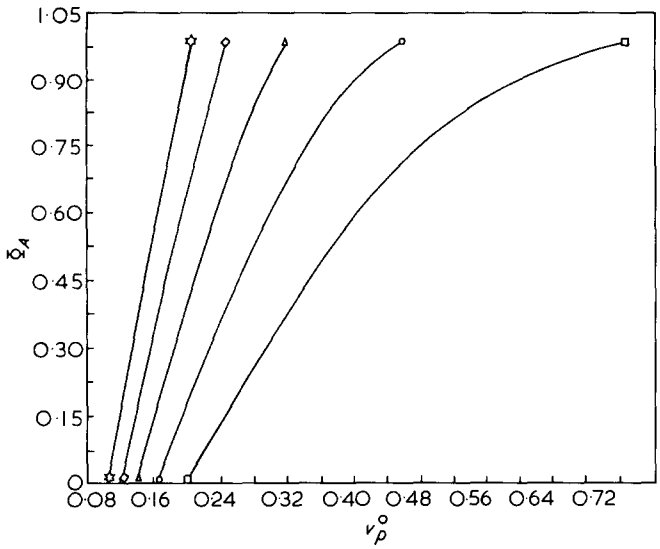

Figure 11 Φ_A against v_p^0 for calculations 'B'. $\Delta\frac{1}{2} = 30$. Lines with extrema as ☆, ◇, △, ○ and □ correspond to x_0 equal to 70, 60, 50, 40, and 30 respectively. Each line gives the bi-phasic range for given (x_0, $\Delta\frac{1}{2}$) pairs. (c.f. *Figure 4*)

species selectively partition into the isotropic phase. *Figure 6* suggests that if one wishes to extract high molecular weight species this is conveniently done by separating-off the anisotropic phase for a bi-phasic material just above the composition v_p^{0*} whilst low molecular weight species are conveniently obtained by separating off the isotropic phase for a bi-phasic material just below the composition v_p^{0**}. *Figure 7* shows the ratio of weight to number average quantities for both phases in the bi-phasic material. As v_p^0 is increased for constant $\Delta\frac{1}{2}$ both $(\bar{x}_p/\langle x_p\rangle)$ and $(\bar{x}'_p/\langle x'_p\rangle)$ increase in magnitude, the variation being far greater for the isotropic material and $(\bar{x}_p/\langle x_p\rangle)$ reaches surprisingly large values.

Figures 8 and *9* show the quantities y and S which give information on the degree of order in the anisotropic phase of the bi-phasic material. In *Figure 9* the values of S are all greater than 0.94 and such high values are characteristic of the Flory model[39]. As v_p^0 increases S shows an initial decrease ('dip') followed by a general increase for the remainder of the bi-phasic range. The magnitude of the dip increases as $\Delta\frac{1}{2}$ is increased but the overall values of S are always increasing with increasing $\Delta\frac{1}{2}$. The initial behaviour is a consequence of the long-length tail of the distribution preferentially seeking the anisotropic phase for v_p^0 close to v_p^{0*} (see also *Figure 6* and discussion above: also note that $(\bar{x}'_p/\langle x'_p\rangle)$ is close to unity (see *Figure 7*) showing that the anisotropic phase has a far lower polydispersity (and hence higher order) than that for the isotropic phase). The partitioning effects for calculations 'A' are most readily seen in *Figure 10* where f_x and f'_x are plotted against x for ($x_0 = 50$, $\Delta\frac{1}{2} = 40$) and for different, but equally spaced, values of v_p^0 (and hence different values of Φ_A). As v_p^0 (and Φ_A) are increased the composition of the bi-phasic material transforms from essentially isotropic to essentially anisotropic phase. The partitioning of the species in terms of molecular weight is clearly seen and the correlation with *Figures 6* and *7* is evident. Curves of the form of *Figure 10* have been given by Flory and co-workers for the 'most-probable' and Poisson distributions.

Calculations 'B'

We consider the results for $\Delta\frac{1}{2}$ fixed at 30 and x_0 varied from 30 to 70. *Figure 11* shows that Φ_A–vs.–v_p^0 curves are successively displaced to higher v_p^0 values and the span of the bi-phasic range is extended as x_0 is decreased. v_p^{0*} and v_p^{0**} decrease with increasing x_0, simply reflecting x_0 and not selective partitioning within the overall distribution, which was an important factor for calculation A, *Figure 4*. In *Figure 12* the values of v_p and v'_p decrease as x_0 is increased for a given value of v_p^0. The partitioning in terms of molecular weight is documented in *Figure 13*. Note here that $\bar{x}_p$ $(v_p^0 \rightarrow v_p^{0*}) \simeq \bar{x}'_p(v_p^0 \rightarrow v_p^{0**})$—as illustrated, for example, by the ★–★ and ☆–☆ extrema—as required on physical grounds. As x_0 decreases the partitioning effect, on the basis of molecular weight, increases. Interestingly $(\bar{x}_p/\langle x_p\rangle)$ values approximate to a single

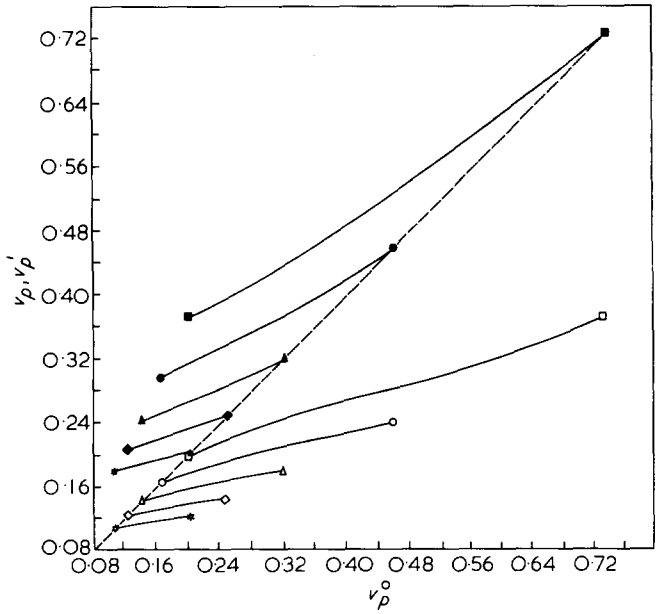

Figure 12 v_p and v'_p against v_p^0 for calculations 'B'. $\Delta\frac{1}{2} = 30$. Open and filled symbols refer to isotropic and anisotropic phases respectively. Key is as in *Figure 11* (c.f. *Figure 5*).

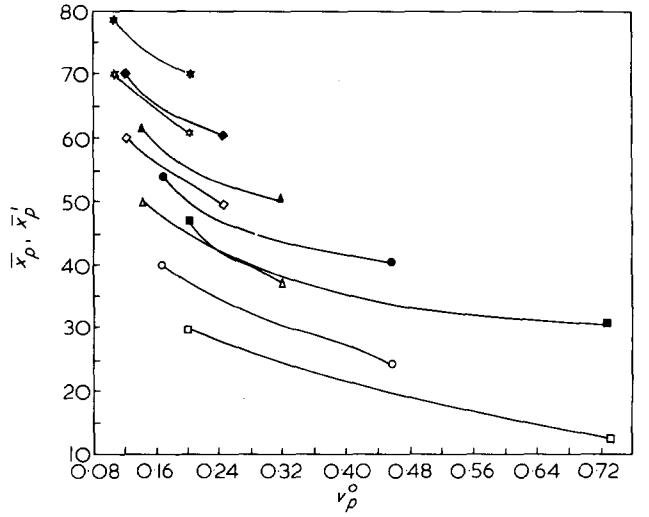

Figure 13 $\bar{x}_p, \bar{x}'_p$ against v_p^0 for calculations 'B'. The lines are constructed, and the notation is the same as for *Figure 12* (c.f. *Figure 6*)

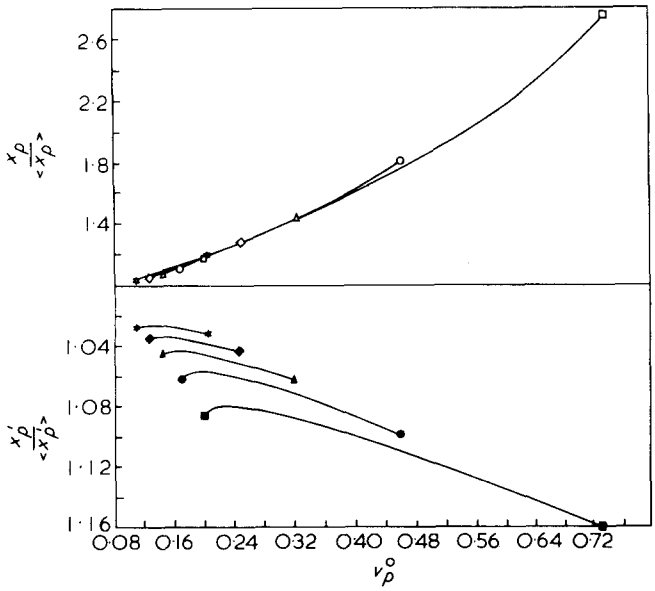

Figure 14 $(\bar{x}_p/\langle x_p\rangle)$ and $(\bar{x}_p'/\langle x_p'\rangle)$ against v_p^0 for calculations 'B'. The lines are constructed, and the notation is the same as for *Figures 12* and *13* (c.f. *Figure 7*)

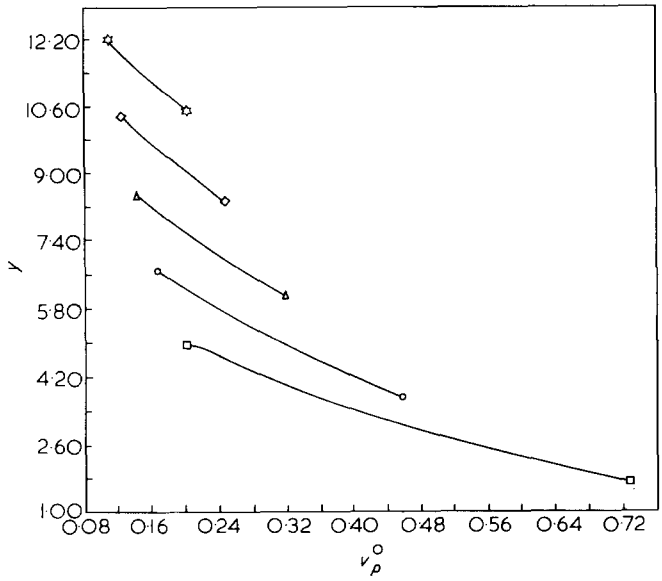

Figure 15 y against v_p^0 for calculations 'B'. The lines are constructed as in *Figure 11* (c.f. *Figure 8*)

curve (in *Figure 14*) whilst $(x_p'/\langle x_p'\rangle)$ curves are displaced as x_0 is decreased. The quantities y and S are shown in *Figures 15* and *16*. Again S shows an initial decrease before its rise (c.f. *Figure 9*). Note that the curves for S successively displace to higher values as x_0 is decreased. As with *Figure 9*, this results from the partitioning of high molecular weight species into the anisotropic phase.

Calculations 'C'

These are complementary to calculations 'B' only now the half-width of the Gaussian is in fixed proportion to x_0, being $\Delta_{\frac{1}{2}}^1 = 2x_0/3$. As is seen in *Figures 2* and *3* the volume fraction distribution functions for the two cases are very different, the higher x_0 is in case 'B', the broader is the curve. As before the curves of Φ_A *Figure 17* displace to higher v_p^0 values as x_0 is decreased and are to be compared with those in *Figure 11*. In *Figure 17* the near parallel curves reflect $\Delta_{\frac{1}{2}}^1$ increasing with x_0 thus maintaining the span of the bi-phasic range whereas in *Figure 11* the transition range narrows with increasing x_0. *Figures 18* and *12* and *Figures 19* and *13* may be compared and note that the differences between $\bar{x}_p'$ and $\bar{x}_p$ are much higher for 'B' than for (C). Comparing *Figures 20* and *14* note that in *Figure 20* whilst all $(\bar{x}_p'/\langle x_p'\rangle)$ values are close to unity, there is a significant decrease in $(\bar{x}_p/\langle x_p\rangle)$ on going from *Figures 14* to *20*. This means that there is a decrease in the tendency to partially fractionate the high molecular weight species into the anisotropic phase for v_p^0 close to v_p^{0*}. *Figures 21* and *22* show y and S, and comparing *Figure 22* with *Figure 16* generally similar curves are obtained. Finally *Figure 23* shows f_x and f_x' against x for equally spaced intervals of v_p^0, for $x_0 = 70$, $\Delta_{\frac{1}{2}}^1 = 2x_0/3$ in

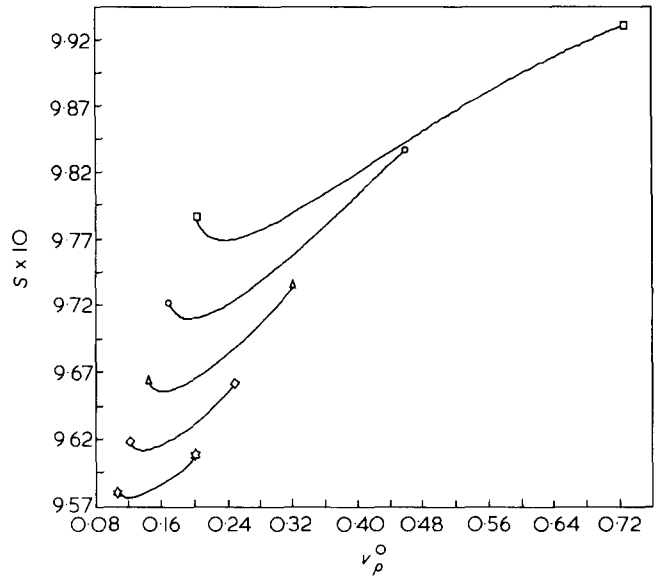

Figure 16 S against v_p^0 for calculations 'B'. The lines are constructed as in *Figure 11* (c.f. *Figure 9*)

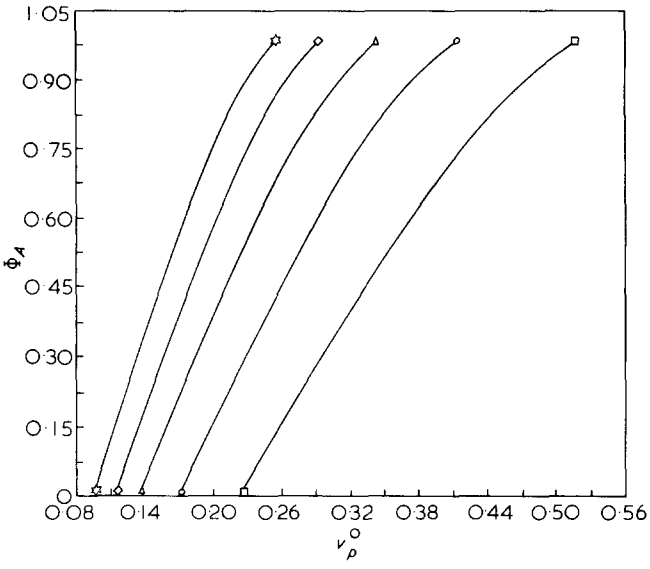

Figure 17 Φ_A against v_p^0 for calculations 'C'. $\Delta_{\frac{1}{2}}^1 = 2x_0/3$. Lines with extrema as ☆, ◇, △, ○, □ correspond to x_0 equal to 70, 60, 50, 40, and 30 respectively. Each line gives the bi-phasic range for given $(x_0, \Delta_{\frac{1}{2}}^1)$ pairs. (c.f. *Figures 4* and *11*)

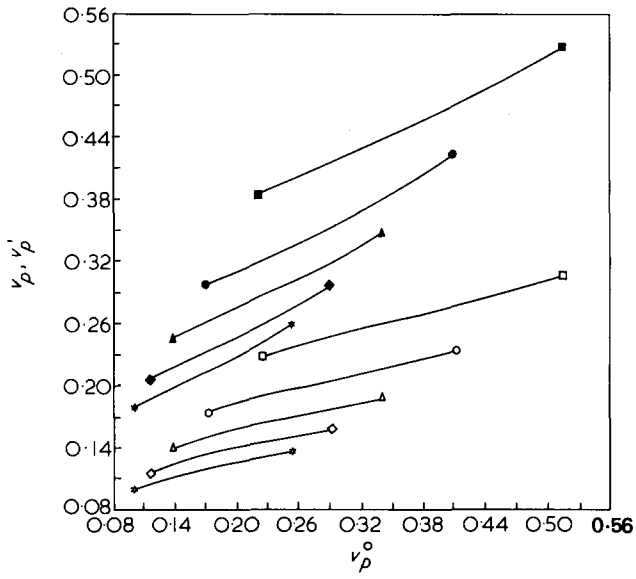

Figure 18 v_p and v_p' against v_p^0 for calculations 'C'. $\Delta_{\frac{1}{2}} = 2x_0/3$. Open and filled symbols correspond to isotropic and anisotropic phases respectively. Key as in *Figure 17* (c.f. *Figures 5* and *12*)

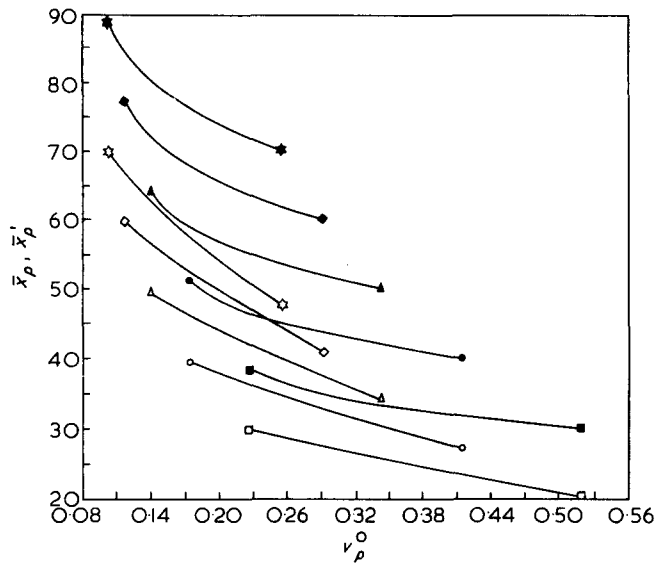

Figure 19 $\bar{x}_p, \bar{x}_p'$ against v_p^0 for calculations 'C'. $\Delta_{\frac{1}{2}} = 2x_0/3$. The lines are constructed as for *Figure 18* (c.f. *Figures 6* and *13*)

the range where Φ_A increases from 0.01 to 0.99 (see *Figure 17*). As in *Figure 10* we observe the partitioning of species into isotropic and anisotropic phases on the basis of molecular weight and we see how the relative amounts $\left(\sum_x f_x'/\sum_x f_x\right)$, and their average molecular weights (see also *Figures 19* and *20*), for the two phases vary with v_p^0 (or Φ_A) in the bi-phasic range.

DISCUSSION

The present work complements the earlier work of Flory and co-workers for polydisperse systems[3-6] and investigates the variations in the derived quantities Φ_A, v_p^{0*}, v_p^{0**}, f_x, f_x', v_p, v_p', average molecular weights and the order parameter S as the width of the distribution ($\Delta_{\frac{1}{2}}$) and x_0 are varied. The effects of varying $\Delta_{\frac{1}{2}}$ are remarkable and have been discussed in detail above. Further interpretations of the curves of *Figures 4–23* could be made but most are self-evident to the reader and thus will not be further discussed. The tabulations of these and other calculations we have made for the Gaussian distribution may be made available on request to the authors, as is the programme for the calculations. The question that arises is to what extent may the above calculations be applicable to our recent experimental dielectric data[32,33,36] for poly(alkylisocyanates) and the viscosity, phase behaviour and thermal data for those systems by Aharoni and co-workers[16-19]?

It appears that the poly(alkylisocyanates) are rod-like for $M_W < 10^5$, as evidenced by a whole range of physical studies[24-31,40], but the chains are worm-like or act as broken rods with large persistence length at the highest molecular weights[24-31,40]. Thus application of the Flory model is likely to be most successful for $M_W < 10^5$ and

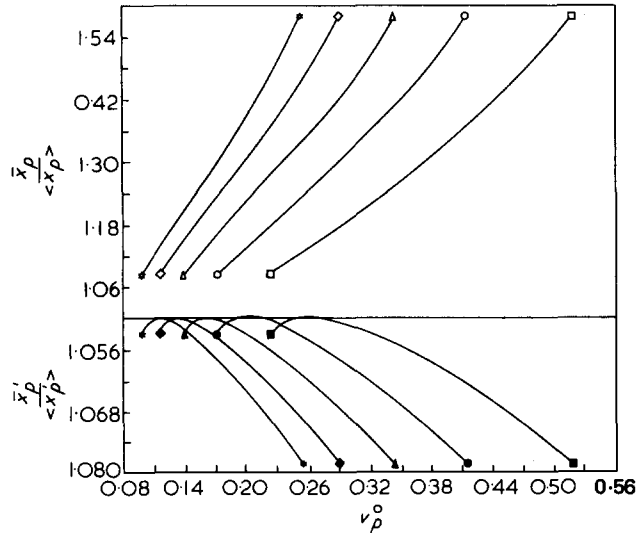

Figure 20 $(\bar{x}_p/\langle x_p \rangle)$ and $(x_p'/\langle x_p' \rangle)$ against v_p^0 for calculations 'C'. The lines are constructed as for *Figures 18* and *19* (c.f. *Figures 7* and *14*)

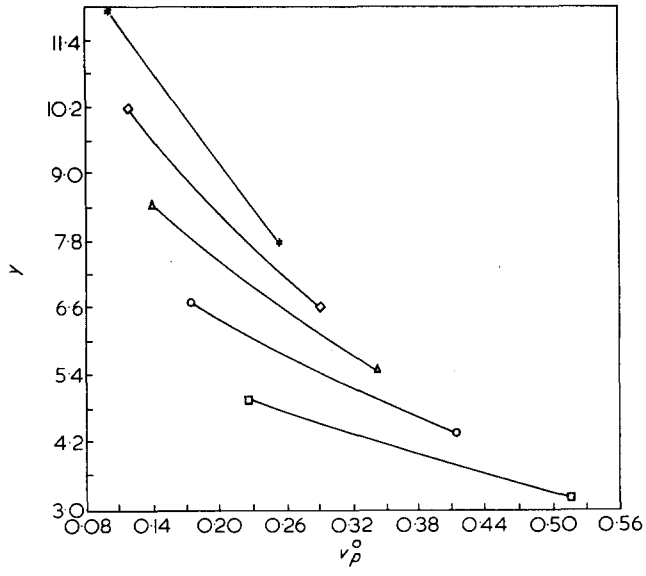

Figure 21 y against v_p^0 for calculations 'C'. The lines are constructed as for *Figure 17* (c.f. *Figures 8* and *15*)

generalization of the theory to include the broken rods, as has been attempted by Flory[7], seems desirable for high molecular weights. Another important aspect is that the Flory model as considered by Flory for polydisperse systems[3-6] and by us here, is derived for athermal solutions: i.e. on the basis of entropy considerations and not including interactions between particles. Since the poly(alkylisocyanates) in solution would be expected to interact *via* their large dipole moments, the athermal approximation may not be adequate, although one would expect the thermal terms to be of considerably smaller magnitude than in, say, polyamide/polar solvent systems where specific interactions (e.g. hydrogen bonding) will be important and will make a substantial contribution to the free energy.

Notwithstanding the reservations expressed above, it is clear from the predictions of the model and the experimental observations of the phase-behaviour and the physical properties of the isotropic, bi-phasic and anisotropic phases of the poly(alkylisocyanates) in non-polar solvents[16-23,32,33,36,40] that the essential experimental features are rationalized, at least semi-quantitatively, by the Flory theory if a distribution of molecular weight is taken into account. We are therefore currently undertaking a simulation of the dielectric properties of a poly(n-hexylisocyanate) in toluene solution extending over the isotropic, bi-phasic and anisotropic phases using the results of the model calculations given above, together with the known dielectric properties of the isolated chain as a function of molecular weight[24-30], and a model of motions in the anisotropic phase due to Warchol and Vaughan[37] and Wang and Pecora[38]. In the latter case it is considered that a rigid dipolar molecule may reorient freely (by small-step diffusion) in a cone described by the polar angle $\theta°$. It follows[37,38] that the mean-square dipole moment $\langle\mu^2\rangle$ and the effective relaxation time $\langle\tau\rangle$ have smaller values for a motion in a cone than for isotropic diffusion into 4π solid angle and this rationalizes the observation[32,33,36] of the fall in static permittivity (ε_0) and the increase in the frequency of maximum loss (f_m) on going from isotropic→bi-phasic→anisotropic phase. Values of θ_x^0 may be inferred from the model calculations described above so it is possible to simulate the dielectric behaviour under athermal conditions for rod-like chains. It remains to be seen if this simulation accounts for the essential features of the observed dielectric behaviour[32,33,36] but qualitative differences should provide further insight into the structure and dynamics of the biphasic and anisotropic phases of poly(alkylisocyanate)/solvent systems.

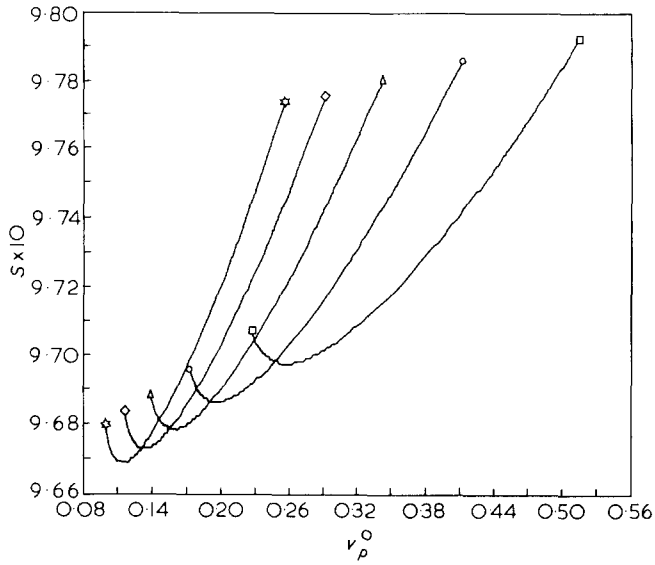

Figure 22 S against v_ρ^0 for calculations 'C'. The lines are constructed as for *Figure 17* (c.f. *Figures 9* and *16*)

ACKNOWLEDGEMENTS

The authors wish to thank the S.R.C. for their support to J.K.M.

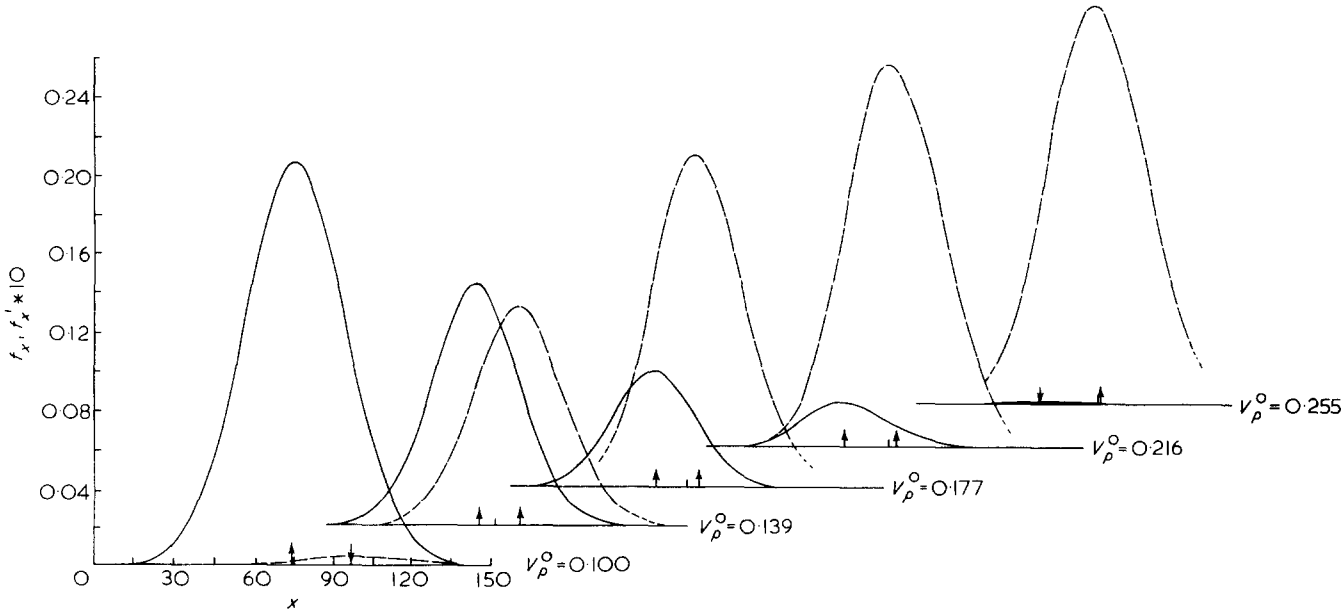

Figure 23 f_x (continuous line) and f'_x (broken line) against x for $x_0 = 70$, $\Delta_1 = 2x_0/3$. Successive plots from left to right refer to v_ρ^0 equal to 0.100 ($\Phi_A = 0.010$), 0.139 ($\Phi_A = 0.348$), 0.177 ($\Phi_A = 0.635$), 0.216 ($\Phi_A = 0.844$) and 0.255 ($\Phi_A = 0.990$). (c.f. *Figure 10*)

GLOSSARY OF TERMS

$\Delta\varepsilon$	dielectric increment across the dipole relaxation region.
$\langle\tau\rangle$	average dielectric relaxation time. $\langle\tau\rangle=(2\pi f_m)^{-1}$ where f_m is the frequency of maximum loss.
c_p	polymer concentration (wt polymer/total weight).
n_x^0, n_p^0	number of x-meric species (n_x^0) in the total number (n_p^0) of polymer species in the unpartitioned system.
v_x^0, v_p^0, V	volume fraction of x-meric species (v_x^0) and volume fraction of all polymer species (v_p^0) in volume V of the unpartitioned system.
$\Delta\frac{1}{2}$	Gaussian curve half-width (see equation (1)).
v_p, v'_p	volume fractions of polymer solute in isotropic phase (v_p) and anisotropic phase (v'_p) of bi-phasic material.
Φ_A	volume fraction of anisotropic phase in volume V of bi-phasic material.
v_x, v'_x	volume fractions of x-meric solute in isotropic phase (v_x) and anisotropic phase (v'_x) of bi-phasic material.
$\bar{x}_p^0$	number average molecular length of polymer in the unpartitioned system (see equation (2)).
$\bar{x}_p$, $\bar{x}'_p$	number average molecular length of polymer in the isotropic phase (unprimed) and anisotropic phase (primed) of the bi-phasic material, respectively.
η, y	see equation (7) and refs. 2–6
$v'_A, v'_R, \bar{x}'_A$ $\bar{x}'_R$	volume fractions and number average. molecular length of polymer solute in the 'aligned' (A) and 'random' (R) parts of the anisotropic phase (hence the prime).
θ_x	$y=x\sin\theta_x$; see equation (7): see also equation (17).
S	order parameter for the anisotropic phase in the bi-phasic material.
$\langle x_p\rangle$, $\langle x'_p\rangle$	weight average molecular length of polymer in the isotropic phase (unprimed) and anisotropic phase (primed) of the bi-phasic material respectively.
v_p^{0*}, v_p^{0**}	volume fractions of the polymer at the beginning (*) and end (**) of the bi-phasic range.
f_x, f'_x	distribution functions for x-meric species in the isotropic (unprimed) and anisotropic (primed) phases of the bi-phasic material (see equation (21)).

REFERENCES

1 Flory, P. J. *Proc. Roy. Soc. (London) A*, 1956, **234**, 73
2 Flory, P. J. *Ber. Bunsenges Phys. Chem.* 1977, **81**, 885
3 Flory, P. J. and Abe, A. *Macromolecules* 1978, **11**, 1119
4 Abe, A. and Flory, P. J. *Macromolecules* 1978, **11**, 1122
5 Flory, P. J. and Frost, R. S. *Macromolecules* 1978, **11**, 1126
6 Frost, R. S. and Flory, P. J. *Macromolecules* 1978, **11**, 1134
7 Flory, P. J. *Macromolecules* 1978, **11**, 1138
8 Flory, P. J. *Macromolecules* 1978, **11**, 1141
9 Dieblieck, R. and Lekkerkerker, H. N. W. *J. Physique (Lett.)* 1980, **41**, 351
10 Doi, M. *J. Polym. Sci., Polym. Phys. Edn.* 1981, **19**, 229
11 Robinson, C. *Trans. Faraday Soc.* 1956, **52**, 571
12 Robinson, C., Ward, J. C. and Beevers, R. B. *Discuss. Faraday Soc.* 1958, **25**, 29
13 Papkov, S. P., Kulichikhin, G. and Kalmykova, V. D. *J. Polym. Sci., Polym. Phys. Edn.* 1974, **12**, 1753
14 Kwolek, S. L., Morgan, P. W., Schaefgen, J. R. and Gulrich, L. W. *Polym. Prepr., Am. Chem. Soc., Div. Polym. Chem.* 1976, **17**, 53
15 Griffen, B. P. and Cox, M. K., *Br.* Polym. J. December, 1980, 147
16 Aharoni, S. M. *Macromolecules* 1979, **12**, 94, 271
17 Aharoni, S. M. and Walsh, E. K. *J. Polym. Sci., Polym. Lett. Edn.* 1979, **17**, 321
18 Aharoni, S. M. and Sibilia, J. P. 20th Canadian High Polymer Forum, August 1979
19 Aharoni, S. M. *Ferroelectrics* 1980, **30**, 227
20 Aharoni, S. M. *Polymer* 1980, **21**, 21
21 Aharoni, S. M. *Polym. Prepr., Am. Chem. Soc., Div. Polym. Chem.* 1980, **21**, 209
22 Aharoni, S. M. *Macromolecules* 1981, **14**, 224
23 Aharoni, S. M. *J. Polym. Sci., Polym. Phys. Edn.* 1980, **18**, 1303, 1439
24 Bur, A. J. and Fetters, L. *Chem. Rev.* 1976, **76**, 727
25 Yu, H., Bur, A. J. and Fetters, L. J. *J. Chem. Phys.* 1966, **4**, 2568
26 Bur, A. J. and Roberts, D. E. *J. Chem. Phys.* 1969, **51**, 406
27 Dev. S. B., Lochhead, R. Y. and North, A. M. *Discuss. Faraday Soc.* 1970, **49**, 244
28 Pierre, J. and Marchal, E. *J. Polym. Sci., Polym. Lett. Edn.* 1975, **13**, 11
29 Coles, H. J., Gupta, A. K. and Marchal, E. *Macromolecules* 1977, **10**, 182
30 Beevers, M. S., Garrington, D. C. and Williams, G. *Polymer* 1977, **18**, 540
31 Jennings, B. R. and Brown, B. L. *Eur. Polym. J.* 1971, **7**, 805
32 Moscicki, J. K., Williams, G. and Aharoni, S. M. *Polymer* 1981, **22**, 571
33 Moscicki, J. K., Williams, G. and Aharoni, S. M. *Polymer* 1981, **22**, 1361
34 Bur, A. J. and Fetters, L. J. *Macromolecules* 1973, **6**, 874
35 Moscicki, J. K. and Williams, G. *Polymer* 1981, **22**, 1451
36 Moscicki, J. K., Williams, G. and Aharoni, S. M. *Macromolecules* in press
37 Warchol, M. P. and Vaughan, W. E. *Adv. Molec. Relax. Interact. Processes* 1978, **13**, 317
38 Wang, C. C. and Pecora, R. *J. Chem. Phys.* 1980, **72**, 5333
39 Warner, M. and Flory, P. J. *J. Chem. Phys.* 1980, **73**, 6327
40 Aharoni, S. M. 27th Int. Symp. Macromol., IUPAC, Strasbourg, 1981, Conf. Abstracts, Vol. II, p. 577–581